

Vision-Language Meets the Skeleton: Progressively Distillation with Cross-Modal Knowledge for 3D Action Representation Learning

Yang Chen, Tian He, Junfeng Fu, Ling Wang, *Member, IEEE*,
Jingcai Guo, *Member, IEEE*, Hong Cheng, *Senior Member, IEEE*

Abstract—Supervised and self-supervised learning are two main training paradigms for skeleton-based human action recognition. However, the former one-hot classification requires labor-intensive predefined action categories annotations, while the latter involves skeleton transformations (e.g., cropping) in the pretext tasks that may impair the skeleton structure. To address these challenges, we introduce a novel skeleton-based training framework (C^2VL) based on Cross-modal Contrastive learning that uses the progressive distillation to learn task-agnostic human skeleton action representation from the Vision-Language knowledge prompts. Specifically, we establish the vision-language action concept space through vision-language knowledge prompts generated by pre-trained large multimodal models (LMMs), which enrich the fine-grained details that the skeleton action space lacks. Moreover, we propose the intra-modal self-similarity and inter-modal cross-consistency softened targets in the cross-modal contrastive process to progressively control and guide the degree of pulling vision-language knowledge prompts and corresponding skeletons closer. These soft instance discrimination and self-knowledge distillation strategies contribute to the learning of better skeleton-based action representations from the noisy skeleton-vision-language pairs. During the inference phase, our method requires only the skeleton data as the input for action recognition and no longer for vision-language prompts. Extensive experiments show that our method achieves state-of-the-art results on NTU RGB+D 60, NTU RGB+D 120, and PKU-MMD datasets. The code will be available in the future.

Index Terms—Action Recognition, Vision-Language, Cross-Modal, Self-Supervised, Contrastive Learning, Large Multimodal Models.

I. INTRODUCTION

ACTION recognition has become a hot topic due to its wide range of application fields, such as human-computer interaction, sports analysis, and dangerous behavior warning [1], etc. In recent years, the continuous development of depth sensors like Kinect [2] has facilitated the easy acquisition of the human body’s skeleton (joints coordinate). Compared with

This work was supported by the National Key Research and Development Program of China (No.2022YFE0133100). (*Corresponding author: Ling Wang.*)

Yang Chen, Junfeng Fu and Ling Wang are with the School of Information and Communication Engineering, University of Electronic Science and Technology of China, Chengdu, China (email: csyachen@std.uestc.edu.cn; junfengfu@std.uestc.edu.cn; eewangling@uestc.edu.cn).

Tian He and Hong Cheng are with the School of Automation Engineering, University of Electronic Science and Technology of China, Chengdu, China (email: tianhe@std.uestc.edu.cn; hcheng@uestc.edu.cn).

Jingcai Guo is with the Department of Computing, The Hong Kong Polytechnic University, Hong Kong SAR, China (email: jc-jingcai.guo@polyu.edu.hk).

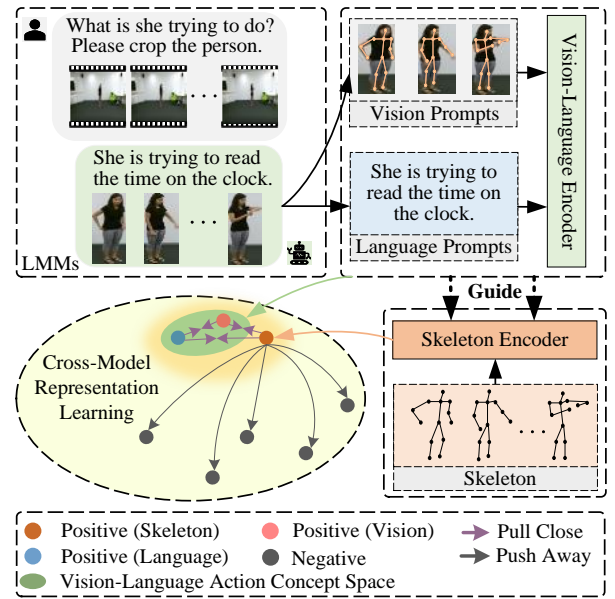


Fig. 1. Our proposed approach (C^2VL) utilizes the vision-language knowledge prompts as supervision to learn task-agnostic 3D human action representations.

RGB-D sequences, the 3D skeleton is naturally robust to light, background noise, and viewpoint changes while also having the advantages of being lightweight and privacy-preserving.

Skeleton-based action recognition methods are primarily categorized into two distinct paradigms: supervised learning and self-supervised learning. In the former, skeleton data serves as the input, with human-designed action category labels represented as one-hot vectors employed for supervision to design complex network architectures [3]–[5]. This training process aims to learn task-specific spatial-temporal representations for actions, which has achieved impressive performance. On the other hand, self-supervised learning approaches generate positive-negative pairs by designing pretext tasks of data transformations (rotation, masking, and cropping, etc.) to explore task-agnostic action representation in a label-free manner based on contrastive learning [6]–[8]. These methods leverage pretext tasks for unsupervised pre-training and then finetune for downstream tasks. The results suggest that the self-supervised approaches have the potential to surpass supervised learning methods.

However, while the abovementioned methods have proven

effective in representing human actions, several challenges remain. (1) Obtaining numerous labeled data is extremely expensive and labor-intensive for supervised learning. Additionally, the reliance on one-hot vector classification restricts the generality of these methods since additional labeled data is needed to address any other tasks. (2) For self-supervised learning, skeleton data transformations (rotation, masking, cropping, etc.) of the pretext task may impair the structural information inherent in skeleton action, leading to information bias. Inspired by the recent success in multi-modal contrastive learning [9]–[11], we consider designing a novel skeleton training paradigm guided by vision-language knowledge to obviate numerous label annotations or compromise the integrity of the skeleton structures, as shown in Fig. 1.

Specifically, our approach leverages sample-specific vision-language knowledge prompts as the supervision to guide the skeleton encoder in learning task-agnostic action representation, which is called C²VL. Firstly, we utilize LMMs (Grounding DINO [12] and LLaVA [13]) as the vision-language engines, employing text prompts and visual questions to generate one-to-one vision knowledge prompts related to human action images and one-to-one language knowledge prompts corresponding to action descriptions, respectively. Subsequently, the vision-language encoders extract features from these knowledge prompts to establish the vision-language action concept space, enriching object-related details and fine-grained descriptions absent in the skeleton action space. However, these one-to-one format skeleton-knowledge pairs exhibit many-to-many correspondences among different samples because LMMs generate similar semantic descriptions for different skeleton actions, which causes the noisy skeleton-vision-language joint action space. Therefore, we introduce the intra-modal self-similarity and inter-modal cross-consistency softened targets in the cross-modal self-knowledge distillation learning to progressively control and guide the degree of bringing vision-language knowledge prompts and corresponding skeletons closer in the noisy joint space. This soft contrastive learning process effectively guides the skeleton encoder to learn better task-agnostic 3D human action representation than the hard alignment in CLIP methods. During the inference phase, only skeleton data is needed as the input for action recognition, and vision-language knowledge prompts are omitted without incurring additional computational costs.

Our contributions can be summarized as follows:

- To the best of our knowledge, this is the first work that utilizes vision-language knowledge prompts as supervision to learn task-agnostic skeleton-based action representations in the training phase. During the inference phase, only the skeleton data is used as the input for skeleton-based action recognition.
- We employ LMMs as the offline vision-language engines to generate vision-language knowledge prompts concerning action descriptions to establish action concept space, which enriches object-related and fine-grained details that the skeleton action space lacked.
- We introduce the intra-modal self-similarity and inter-modal cross-consistency softened targets to relax the strict one-to-one constraint, effectively guiding the instance

discrimination and knowledge distillation process in the noisy joint action space.

- Extensive experiments show the superior performance of our training paradigm on the NTU RGB+D 60, NTU RGB+D 120, and PKU-MMD datasets. Notably, our self-supervised method even surpasses some supervised learning methods and has a significant margin improvement under semi-supervised learning scenarios.

II. RELATED WORK

In this section, we mainly introduce the related work of skeleton-based action recognition, multi-modal representation learning, and vision-language pretraining with noisy data.

A. Skeleton-based Action Recognition

Supervised skeleton-based action recognition has been the dominant paradigm. CNN-based approaches [14], [15] transform skeleton data into image-like structures, and RNN-based methods [16], [17] delve into long-term contextual relationships from joint sequences, both of them ignore the skeleton's inherent graph topology. GCN-based methods [3], [4], [18] regard human joints and bones as graph nodes and edges, respectively, enabling effective exploration of the spatial-temporal representation of actions while keeping structural properties. However, the above-mentioned supervised approaches have the disadvantage of requiring extensive human-designed category annotations. Much research pays attention to self-supervised approaches, which are adept at learning task-agnostic representation in a label-free manner. Reconstruction and contrastive learning are two main problem-solving concepts. They reconstruct skeleton structures by masked modeling [19]–[22] or generate positive-negative pairs [6]–[8], [23], [24] through skeleton transformation (e.g., rotation, cropping) respectively to explore action representation. Unfortunately, these pretext tasks impair the topological structure of the skeleton, leading to information bias. [Summary]: In this paper, we first explore the possibility of learning action representation for skeleton-based action recognition from other modalities (vision and language) without label annotation or skeleton damage.

B. Multimodal Representation Learning

Numerous multimodal approaches have demonstrated the capacity to learn powerful representations from different modalities. Inspired by their success, foundational vision-language models such as CLIP [9] and ALIGN [25] have gained widespread adoption in the domain of RGB-based action recognition [1], [10], [11], [26]–[31]. Many approaches rely on human-designed coarse-grained category names for video action classification [10], pose estimation [28] and action generation [29], etc. Much recent research gradually employs LLMs (GPT-3, etc.) to generate detailed action descriptions of category names for RGB-based action classification [30] and generation [31]. GAP [11] is the first work to utilize LLMs (GPT-3) for skeleton-based action recognition. Regrettably, although these approaches enrich category names with meaningful semantics, the relationship between each action

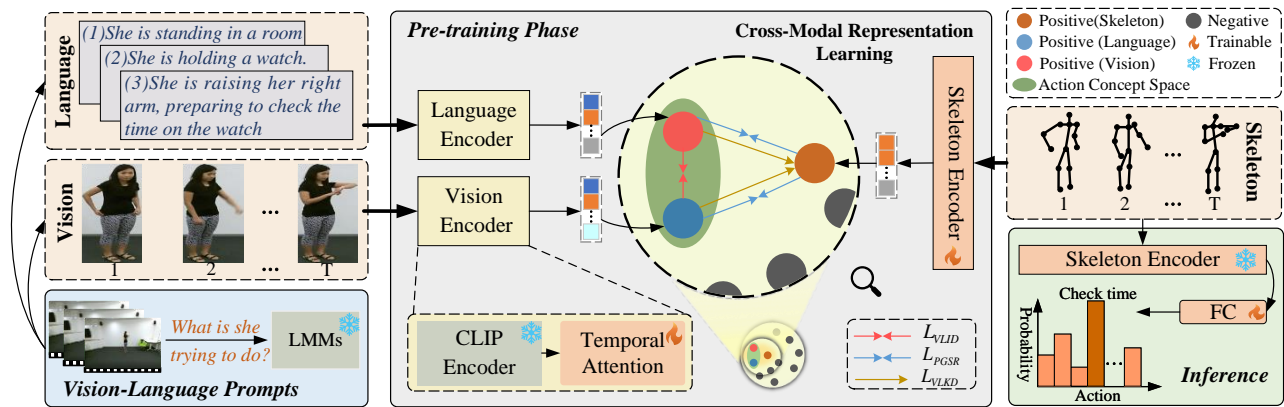


Fig. 2. The pipeline of our proposed approach. Before the pre-training phase, the vision and language knowledge prompts are generated regarding skeleton sequences by offline LMMs (Grounding DINO [12] and LLaVA [13]) with text prompts and visual questions. In the pre-training phase, the skeleton data is utilized as the input for the skeleton encoder to learn action representation in the skeleton action space. The vision encoder and language encoder are employed to extract features from vision and language knowledge prompts, contributing to the creation of the vision-language action concept space that enhances fine-grained details not captured in the skeleton space. Subsequently, the degree to which pairs consisting of vision-language knowledge prompts and their corresponding skeleton are brought closer should be progressively guided by the intra-modal self-similarity and inter-modal cross-consistency softened targets. During the inference phase, we only utilize the former pre-trained skeleton encoder with a fully connected layer and skeleton data for skeleton-based action recognition without vision-language knowledge prompts.

description and skeleton sample falls under the one-to-many format, which belongs to the supervised learning paradigm. [Summary]: In contrast, our proposed framework differs in two aspects. Firstly, we leverage LMMs (Grounding DINO [12] and LLaVA [13]) as offline engines to generate sample-level vision-language knowledge prompts in a one-to-one format without requiring labor-intensive annotations. Second and more importantly, we utilize these one-to-one vision-language knowledge prompts as the supervisory signal to learn skeleton representation in a self-supervised learning paradigm.

C. Contrastive Learning with Noisy Pairs

Contrastive learning is the core of the recent multimodal self-supervised learning methods, which pulls the positive pairs closer and pushes the negative pairs away [32], [33]. However, the noisy many-to-many correspondences existed in the label-intensive annotated and web-collected pairs, showing the potential semantic similarity between negative samples. This phenomenon leads to the computational inefficiency of the conventional contrast process that pursues the hard alignment [34]. Therefore, several techniques have been developed from the soft alignment perspective to learn robust representations from noisy pairs [34]–[39], including the weighting mechanism [35], [36], k-nearest neighbors scheme [39], and knowledge distillation as softening targets [34], [37], [38]. [Summary]: In this paper, we design two softened targets with the self-distillation mechanism to progressively mitigate the adverse effects of noisy pairs and refine inconsistent alignment for more coherent representations.

III. METHOD

In this section, we begin with an introduction to generating vision-language knowledge prompts (Section III-A). Following that, we describe the contrastive learning process with InfoNCE loss (Section III-B). Then, we introduce two

soft targets (Section III-C). Finally, the progressive training objectives with dynamic mechanisms are described (Section III-D). The pipeline of the method is shown in Fig. 2.

A. Vision-Language Action Concept Space

For a given skeleton dataset $D \in \{S_i\}_{i=1}^{|D|}$, we first generate the sample-level vision-language knowledge prompts $\{(V_i, L_i)\}_{i=1}^{|D|}$ by offline LMMs (Grounding DINO [12] and LLaVA [13]). These sample-level vision-language knowledge prompts have a one-to-one corresponding with skeleton sequence, which establishes the vision-language action concept space as shown in Fig. 3.

1) *Vision Knowledge Prompts*: To the best of our knowledge, prior skeleton-based action recognition methods have yet to explore the possibility of utilizing videos to guide the learning of skeleton representation. Here, we introduce the video modality to enrich the motion patterns and object-related details of skeleton representation. These raw videos and skeleton sequences have one-to-one correspondence as they are captured simultaneously by Kinect devices. However, raw videos are challenged to capture fine-grained details and subtle movement changes because of interference from irrelevant background environments. To mitigate this issue, we leverage a pre-trained open-set object detector called Grounding DINO [12], with text prompts “*person*” to crop the human action images as vision knowledge prompts precisely. These vision knowledge prompts only consist of human action regions enhancing the motion patterns in the vision action concept space.

2) *Language Knowledge Prompts*: Inspired by the success of CLIP in handling image-text pairs, numerous methods [10], [11], [28], [29] employ human-designed action names and LLMs-generated movement descriptions for action recognition. However, this language information is at the category level and has a one-to-many relationship with the skeleton

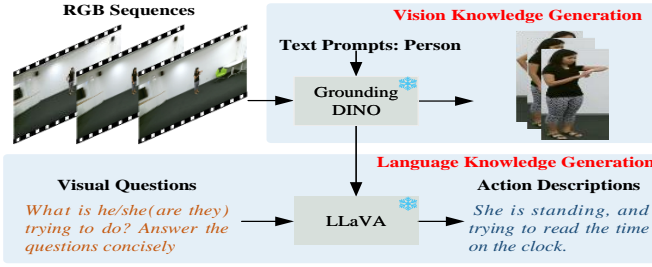


Fig. 3. The establishment of vision-language action concept space.

sequences, so more sample-specific detail descriptions are needed. Therefore, we aim to establish sample-level language action descriptions to enrich the action concept space without requiring expensive annotation and labor-intensive effort. Fortunately, LMMs have an advantage in visual question answering, presenting a new opportunity. Here, we utilize LLaVA [13] with suitable question prompts “*Is he/she or are they holding anything in the hand? Is he/she or are they standing or sitting? What is he/she or are they trying to do? Answer the questions concisely*” to comprehend and generate action descriptions to the vision action images autonomously. These language knowledge prompts provide sample-specific fine-grained detail descriptions in the language action concept space.

B. Contrastive Learning with InfoNCE Loss

Consider a batch of B paired skeleton-vision-language tuples $\{(S_i, V_i, L_i)\}_{i=1}^B$ drawn from the above-mentioned multi-modal space, we aim to learn skeleton encoders E_s based on cross-modal contrastive learning. Specifically, for the i -th pair, the skeleton data S_i , vision data V_i and language data L_i are input into the skeleton encoder E_s , vision encoder E_v and language encoder E_t respectively to get the corresponding modality features. Then, various projectors map these features to a shared latent space for generating L2-normalized embedding pairs $\{(s_i, v_i, l_i)\}_{i=1}^B$, where $s_i, v_i, l_i \in \mathbb{R}^d$. We use the InfoNCE [40] loss to align the skeleton and vision spaces, which focuses on maximizing the similarity between s_i and v_i to pull the paired skeleton-vision embeddings together in two directions. The loss \mathcal{L}_{s2v} for aligning skeleton to vision is defined as follows:

$$\mathcal{L}_{s2v} = -\frac{1}{B} \sum_{i=1}^B \log \frac{\exp(\text{sim}(s_i, v_i)/\tau)}{\sum_{j=1}^B \exp(\text{sim}(s_i, v_j)/\tau)}, \quad (1)$$

where $\text{sim}(\cdot)$ denotes the cosine similarity, and τ is the learnable temperature parameter. The alignment process between these two spaces can be denoted as $\mathcal{L}_{\text{infoNCE}}^{sv} = \mathcal{L}_{s2v} + \mathcal{L}_{v2s}$, and the definition of \mathcal{L}_{v2s} is similar to the \mathcal{L}_{s2v} . For convenience, we simplify and re-write the loss in the matrix as:

$$\mathcal{L}_{\text{infoNCE}}^{sv} = \mathcal{H}(\mathbf{I}_B, \rho(\mathbf{S}\mathbf{V}^T)) + \mathcal{H}(\mathbf{I}_B, \rho(\mathbf{V}\mathbf{S}^T)), \quad (2)$$

$$\mathcal{L}_{\text{infoNCE}}^{sl} = \mathcal{H}(\mathbf{I}_B, \rho(\mathbf{S}\mathbf{L}^T)) + \mathcal{H}(\mathbf{I}_B, \rho(\mathbf{L}\mathbf{S}^T)), \quad (3)$$

where \mathcal{H} is the cross-entropy function, and ρ is the standard softmax function. The \mathbf{I}_B is the identity matrix, and $\mathbf{S}, \mathbf{V}, \mathbf{L} \in$

$\mathbb{R}^{B \times d}$ are the matrices that contain a batch of skeleton, vision and language embeddings. Besides, we align the skeleton and language space similarly by minimizing the $\mathcal{L}_{\text{infoNCE}}^{sl}$.

In practice, the strict assumption in InfoNCE loss to bring (s_i, v_i, l_i) closer and push (s_i, v_j, l_k) away is unreasonable for two reasons. First, as shown in Fig. 4, the ground truth vision-language knowledge prompts (v_i, l_i) of the given skeleton s_i may be incorrect because of hallucination in LMM and poor pose estimation, showing low semantic similarity scores among positive pairs. Second, as shown in Fig. 5, the given skeleton s_i would be aligned to unpaired vision-language knowledge prompts (v_j, l_k) with shared semantics to different degrees within a larger batch size, resulting in high similarity semantic scores among negative pairs. For these, the three modality pairs exhibit many-to-many correspondences among different samples in a batch. The hard alignment between these spaces based on InfoNCE loss will result in poor skeleton representations, as shown in Fig. 7a and Fig. 7c.

C. Cross-modal Alignment with Soft Targets

To address the limitations of using standard InfoNCE loss to learn skeleton representation on noisy joint action concept space, we attempt to design two soft targets to guide the learning of cross-modal alignment. These soft targets play crucial roles in repairing a sample with more semantically similar correspondences in other modalities, which relaxes the explicit one-to-one correspondences and improves the implicit many-to-many relationships.

1) *Intra-modal Self-similarity Guidance*: To estimate the many-to-many relationships within (s_i, v_j, l_k) , we propose to utilize the intra-modal self-similarity to guide the learning of skeleton representation from the vision-language knowledge prompts. Specifically, we calculate the skeleton-to-skeleton similarity $\mathbf{S}\mathbf{S}^T$, vision-to-vision similarity $\mathbf{V}\mathbf{V}^T$, and language-to-language similarity $\mathbf{L}\mathbf{L}^T$ in their respective modality space as soft labels. For the training stability, we use the weighted average strategy [37] to fuse the hard and soft labels as the softened targets to supervise the skeleton-to-vision, vision-to-skeleton, skeleton-to-language, and language-to-skeleton correspondences, respectively. These intra-modal self-similarity softened targets within a batch are defined as follows:

$$\mathbf{P}^{v2s} = \beta \rho(\mathbf{V}\mathbf{V}^T) + (1 - \beta) \mathbf{I}_B, \quad (4)$$

$$\mathbf{P}^{l2s} = \beta \rho(\mathbf{L}\mathbf{L}^T) + (1 - \beta) \mathbf{I}_B, \quad (5)$$

$$\mathbf{P}^{s2v}, \mathbf{P}^{s2l} = \beta \rho(\mathbf{S}\mathbf{S}^T) + (1 - \beta) \mathbf{I}_B, \quad (6)$$

where β is a trade-off hyper-parameter set to 0.2. After replacing the hard targets \mathbf{I}_B with softened targets $\mathbf{P}_{\text{intra}}^{sv}$, $\mathbf{P}_{\text{intra}}^{vs}$, $\mathbf{P}_{\text{intra}}^{sl}$ and $\mathbf{P}_{\text{intra}}^{ls}$, the model can control the degree of attractive and repulsive forces between the skeleton and vision-language embeddings based on their intra-modal self-similarity for more generalized skeleton representation.

2) *Inter-modal Cross-consistency Boosting*: Although the intra-modal self-similarity relaxes the one-to-one constraint and pursues the many-to-many correspondences among the three modalities, the confidence value of the original positive pairs is still at the domination position. Especially for those

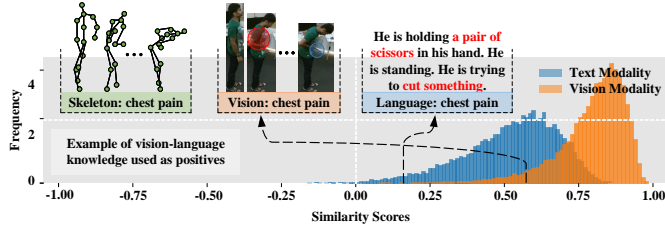


Fig. 4. Histogram of similarity scores for positive pairs between skeleton and vision-language knowledge representations in cross-modal space after training with original infoNCE loss.

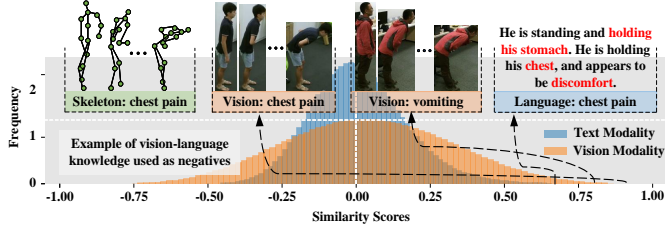


Fig. 5. Histogram of similarity scores for negative pairs between skeleton and vision-language knowledge representations in cross-modal space after training with original infoNCE loss. The red ellipse highlights the movement of arms.

faulty positive pairs, the higher confidence may restrain and submerge the process of repairing samples with more semantically similar correspondences. To mitigate this issue, we adopt the cycle consistent prediction strategy [36] to generate the inter-nodal cross-consistency soft targets as defined as follows:

$$\mathbf{Q}^{v2s} = \rho(\mathbf{SV}^T + \mathbf{I}_B \mathbf{VS}^T \mathbf{J} + \mathbf{JS}^T \mathbf{VI}_B), \quad (7)$$

$$\mathbf{Q}^{s2v} = \rho(\mathbf{VS}^T + \mathbf{I}_B \mathbf{SV}^T \mathbf{J} + \mathbf{JV}^T \mathbf{SI}_B), \quad (8)$$

$$\mathbf{Q}^{l2s} = \rho(\mathbf{SL}^T + \mathbf{I}_B \mathbf{LS}^T \mathbf{J} + \mathbf{JS}^T \mathbf{LI}_B), \quad (9)$$

$$\mathbf{Q}^{s2l} = \rho(\mathbf{LS}^T + \mathbf{I}_B \mathbf{SL}^T \mathbf{J} + \mathbf{JL}^T \mathbf{SI}_B), \quad (10)$$

where \mathbf{J} is an all-one matrix. The first term of Equation 7-10 aggregates the information from its cross opposite modality for dual-direction alignment, *i.e.*, alignment from vision \mathbf{v}_i to skeleton \mathbf{s}_j is based on the probability that skeleton \mathbf{s}_i matched with vision \mathbf{v}_j . Moreover, the second and third terms are designed to avoid positive pairs that are not sound correspondences for boosting negative pairs with high semantic similarity in cross-modalities.

D. Progressive Self-distillation Training Objectives

Here, we introduce a progressive self-knowledge distillation framework [41] where the two soft targets are dynamically updated at each epoch by the teacher network to guide the learning of the student network. Compared to the conventional knowledge distillation methods utilized the static and separate pre-trained teacher network, the main difference of this self-distillation strategy is that it regards the same model architecture as the student and teacher, which has the advantage of reducing computation and memory costs. Meanwhile, as the training goes on, the well-trained teacher can provide more confidence in learning soft labels for students, which

mitigates the adverse effects of noisy pairs and enhances the generalization capability.

To align skeleton space with vision-language spaces, we adopt a progressive scheme [34] to gradually control and balance the roles of two soft targets throughout training. Specifically, we partition a batch of pairs into two subsets with the refreshed hyper-parameter $\alpha \in [0, 1]$ at each epoch. The intra-modal self-similarity soft target is utilized to repair the first subset data $\mathbf{B}_{\text{intra}} = \lfloor \alpha \mathbf{B} \rfloor$ for estimation of the many-to-many relationships, while the inter-class modal cross-consistency is employed to guide the second subset data $\mathbf{B}_{\text{inter}} = \mathbf{B} - \lfloor \alpha \mathbf{B} \rfloor$ for boosting negative pairs with high semantic similarity. At the initial training phase, the value of α should be large for training stability. With the increased training iterations, we gradually decrease the value of α by cosine annealing schedule [42] to increase the contribution of alignment extent between skeleton and high semantic similarity vision-language knowledge prompts. The start value is 0.9, and the end value is 0.1. In this way, the skeleton representation can be better learned in the noisy cross-modal pairs.

Altogether, the final training objective can be formulated as follows:

$$\mathcal{L}_{\text{Soft}} = \mathcal{L}_{\text{Soft}}^{sv} + \mathcal{L}_{\text{Soft}}^{sl}, \quad (11)$$

$$\begin{aligned} \mathcal{L}_{\text{Soft}}^{sv} = & \alpha [\mathcal{H}(\mathbf{P}_{\text{intra}}^{s2v}, \rho(\overline{\mathbf{S}}\mathbf{V}^T)) + \mathcal{H}(\mathbf{P}_{\text{intra}}^{v2s}, \rho(\overline{\mathbf{V}}\mathbf{S}^T))] + \\ & (1 - \alpha) [\mathcal{H}(\mathbf{Q}_{\text{inter}}^{s2v}, \rho(\mathbf{S}\mathbf{V}^T)) + \mathcal{H}(\mathbf{Q}_{\text{inter}}^{v2s}, \rho(\mathbf{V}\mathbf{S}^T))], \end{aligned} \quad (12)$$

$$\begin{aligned} \mathcal{L}_{\text{Soft}}^{sl} = & \alpha [\mathcal{H}(\mathbf{P}_{\text{intra}}^{s2l}, \rho(\overline{\mathbf{S}}\mathbf{L}^T)) + \mathcal{H}(\mathbf{P}_{\text{intra}}^{l2s}, \rho(\overline{\mathbf{L}}\mathbf{S}^T))] + \\ & (1 - \alpha) [\mathcal{H}(\mathbf{Q}_{\text{inter}}^{s2l}, \rho(\mathbf{S}\mathbf{L}^T)) + \mathcal{H}(\mathbf{Q}_{\text{inter}}^{l2s}, \rho(\mathbf{L}\mathbf{S}^T))], \end{aligned} \quad (13)$$

where $\mathbf{P}_{\text{intra}}^*$ is the first $\mathbf{B}_{\text{intra}}$ rows of intra-modal self-similarity soft targets, and the $\mathbf{Q}_{\text{inter}}^*$ is the last $\mathbf{B}_{\text{inter}}$ rows of inter-modal cross-consistency soft targets. $\overline{\mathbf{S}}, \overline{\mathbf{V}}, \overline{\mathbf{L}} \in \mathbb{R}^{\mathbf{B}_{\text{intra}} \times d}$ denotes the first $\mathbf{B}_{\text{intra}}$ rows of skeleton, vision, and language embeddings, respectively. Meanwhile, $\underline{\mathbf{S}}, \underline{\mathbf{V}}, \underline{\mathbf{L}} \in \mathbb{R}^{\mathbf{B}_{\text{inter}} \times d}$ denotes the last $\mathbf{B}_{\text{inter}}$ rows of respective embeddings.

In the inference phase, only the skeleton sequences and encoder E_s are used for skeleton-based action recognition. The vision-language prompts and respective encoders will be dropped.

IV. EXPERIMENTS

A. Datasets

1) *NTU RGB+D 60 Dataset* [43]: It comprises 60 predefined action categories and 56,880 action samples, containing multiple modalities, including RGB, depth map, skeleton, and infrared (IR) video. The skeleton sequences contain a maximum of two human skeletons, represented by the 3D coordinates of 25 joints. The RGB video has a resolution of 1920×1080 . Two benchmarks are provided in this dataset: cross-subject (Xsub) and cross-view (Xview). In Xsub, 20 subjects are used for training, while the remaining subjects are used for testing. In Xview, sequences from views 2 and 3 are designated for training, and the sequences from view 1 are used for testing.

TABLE I

COMPARISON TO THE STATE-OF-THE-ART METHODS FOR ACTION RECOGNITION ON THE NTU RGB+D 60, NTU RGB+D 120, AND PKU-MMD II DATASETS UNDER THE LINEAR EVALUATION PROTOCOL. THE BEST AND SECOND-BEST RESULTS ARE HIGHLIGHTED IN **BOLD** AND UNDERLINED, RESPECTIVELY. THE J REFERS TO THE JOINT MODALITY, THE M DENOTES THE MOTION MODALITY, AND THE B IS THE BONE MODALITY.

Method	Publication	Architecture	Modality	NTU60		NTU120		PKU-MMD II
				xsub	xview	xsub	xset	xsub
<i>Single-stream:</i>								
AimCLR [39]	AAAI'22	GCN	J	74.3	79.7	63.4	63.4	-
CPM [46]	ECCV'22	GCN	J	78.7	84.9	68.7	69.6	48.3
CMD [47]	ECCV'22	GRU	J	79.8	86.9	70.3	71.5	43.0
HaLP [48]	CVPR'23	GRU	J	79.7	86.8	71.1	72.2	43.5
ActCLR [8]	CVPR'23	GCN	J	80.9	86.7	69.0	70.5	-
DMMG [49]	TIP'23	GCN	J	82.1	87.1	69.6	70.1	-
CSTCN [23]	TMM'23	GRU	J	83.1	88.7	72.5	77.4	48.0
UmURL [50]	ACM MM'23	Transformer	J	82.3	<u>89.8</u>	73.5	74.3	<u>52.1</u>
PCM ³ [51]	ACM MM'23	GRU	J	<u>83.9</u>	90.4	76.5	<u>77.5</u>	51.5
KTCL [24]	TMM'24	Transformer	J	82.4	89.4	74.4	74.5	-
C²VL (Ours)	This work	GCN	J	84.4	<u>89.8</u>	<u>76.0</u>	78.7	52.6
<i>Multi-stream:</i>								
3s-CrosSCLR [6]	CVPR'21	GCN	J+M+B	77.8	83.4	67.9	66.7	21.2
3s-AimCLR [39]	AAAI'22	GCN	J+M+B	78.9	83.8	68.2	68.8	39.5
3s-CMD [47]	ECCV'22	GRU	J+M+B	84.1	90.9	74.7	76.1	52.6
3s-CPM [46]	ECCV'22	GCN	J+M+B	83.2	87.0	73.0	74.0	51.5
3s-ActCLR [8]	CVPR'23	GCN	J+M+B	84.2	88.8	74.3	75.7	-
2s-DMMG [49]	TIP'23	GCN	J+M	84.2	89.3	72.7	72.4	-
3s-CSTCN [23]	TMM'23	GRU	J+M+B	85.8	92.0	77.5	78.5	53.9
3s-UmURL [50]	ACM MM'23	Transformer	J+M+B	84.4	91.4	75.9	77.2	54.3
3s-PCM ³ [51]	ACM MM'23	GRU	J+M+B	<u>87.4</u>	93.1	80.0	81.2	58.2
3s-C²VL (Ours)	This work	GCN	J+M+B	88.3	<u>92.8</u>	82.5	84.3	60.0

2) *NTU RGB+D 120 Dataset [44]*: It is an extension of NTU RGB+D 60 with 120 predefined action categories and 114,480 action samples, which have the same modality as NTU RGB+D 60. Similarly, this dataset provides two benchmarks: cross-subject (Xsub) and cross-setup (Xset). In Xsub, sequences from 53 subjects are utilized for training, while the remaining subjects are reserved for testing. In Xset, sequences from even camera IDs are designated for training, and the rest are employed for testing.

3) *PKU-MMD Dataset [45]*: It comprises 51 action categories and almost 20000 action samples with the same multi-modalities as the NTU series datasets. The dataset also provides two benchmarks: cross-subject (Xsub) and cross-view (Xview). In Xsub, sequences from 57 subjects belong to the training set and 9 subjects for the testing. In Xview, sequences from the middle and right views are utilized for training, and the left is used for testing. In this experiment, we adopt the cross-subject benchmark following the previous studies.

B. Implementation Details

All experiments are conducted using the PyTorch framework on an NVIDIA A100 GPU. Each sample is down-sampled to 64 frames using the data pre-processing code from [11]. We use ST-GCN [52] as our skeleton GCN encoder. For the image-text encoder, we utilize the pre-trained **ViT-L/14@336px** model from CLIP [9] and freeze its parameters during training. The temperature parameter τ is 0.07. In the pre-training phase, we train the model with the SGD optimizer for 150 epochs with a batch size 400. The initial learning rate is 0.1 and reduced by a factor of 0.1 at epochs 130 and 140. Weight decay is set to 5e-4 following the strategy in

[11]. In the inference stage, we utilize multiple evaluation protocols, including the linear evaluation protocol, finetune protocol, semi-supervised evaluation protocol(1%, 5% or 10% labeled data), KNN evaluation protocol, and transfer learning evaluation protocol for action recognition.

C. Comparison to the State-of-the-art

To comprehensively evaluate the performance of our method, we conduct comparisons with other state-of-the-art methods across various settings.

1) *Linear Evaluation*: The linear evaluation protocol applies a fully connected layer after the parameter-fixed ST-GCN to classify. As shown in Table I, we found that both single-stream and three-stream performance can achieve the best or the second-best results on NTU RGB+D 60 & 120 and PKU-MMD II datasets, indicating that vision-language knowledge prompts have a solid capacity to guide GCN for generalization representation.

2) *Finetune Evaluation*: We pre-train ST-GCN and finetune the entire network for action recognition, applying a fully connected layer. Table II compares the results obtained through our pre-training and other training paradigms. Notably, our training paradigm performs better in capturing action patterns and details from vision-language knowledge prompts, outperforming some supervised learning methods (Shift-GCN) and even surpassing state-of-the-art self-supervised methods.

3) *Semi-supervised Evaluation*: Our approach involves pre-training with the entire training data and finetuning the classifier with only 1%, 5%, and 10% of the labeled data, respectively. Table III demonstrates that our method significantly renews the accuracy of the state-of-the-art methods, indicating

TABLE II

COMPARISON OF ACTION RECOGNITION RESULTS EMPLOYING DIFFERENT TRAINING PARADIGMS (SUPERVISED AND SELF-SUPERVISED LEARNING) ON THE NTU DATASET. SUPERVISED LEARNING UTILIZES ONE-HOT LABELS FOR TRAINING MODELS, WHILE SELF-SUPERVISED LEARNING UTILIZES THE PRETEXT TASK TO PRE-TRAIN MODELS AND FINE-TUNE THEM WITH LABELS. THE BEST AND SECOND-BEST RESULTS ARE HIGHLIGHTED IN **BOLD** AND UNDERLINED, RESPECTIVELY. SL: SUPERVISED LEARNING, SSL: SELF-SUPERVISED LEARNING.

Method	Paradigm	NTU60		NTU120	
		xsub	xview	xsub	xset
<i>Single-stream:</i>					
ST-GCN [52]	SL	81.5	88.3	70.7	73.2
Shift-GCN [53]	SL	87.8	95.1	80.9	83.2
SkeletonCLR [6]	SSL	<u>82.2</u>	<u>88.9</u>	<u>73.6</u>	<u>75.3</u>
AimCLR [39]	SSL	83.0	89.2	77.2	76.1
CPM [46]	SSL	84.8	91.1	78.4	78.9
ActCLR [8]	SSL	<u>85.8</u>	<u>91.2</u>	<u>79.4</u>	<u>80.9</u>
C²VL (Ours)	SSL	88.9	93.2	83.4	84.9
<i>Multi-stream:</i>					
3s-ST-GCN [52]	SL	85.2	91.4	77.2	77.1
4s-Shift-GCN [53]	SL	90.7	96.5	85.9	87.6
3s-CrosSCLR [6]	SSL	<u>86.2</u>	<u>92.5</u>	<u>80.5</u>	<u>80.4</u>
3s-AimCLR [39]	SSL	86.9	92.8	80.1	80.9
3s-ActCLR [8]	SSL	<u>88.2</u>	<u>93.9</u>	<u>82.1</u>	<u>84.6</u>
3s-C²VL (Ours)	SSL	91.8	95.7	87.8	89.2

TABLE III

COMPARISON OF ACTION RECOGNITION RESULTS UNDER SEMI-SUPERVISED EVALUATION PROTOCOL ON NTU RGB+D 60 DATASET. THE BEST AND SECOND-BEST RESULTS ARE HIGHLIGHTED IN **BOLD** AND UNDERLINED, RESPECTIVELY.

Method	xsub			xview		
	1%	5%	10%	1%	5%	10%
ASSL [54]	-	57.3	64.3	-	63.6	69.8
MS ² L [55]	33.1	-	65.1	-	-	-
MCC [56]	-	47.4	60.8	-	53.3	65.8
ISC [57]	35.7	59.6	65.9	38.1	65.7	72.5
Colorization [19]	48.3	65.7	71.7	52.5	70.3	78.9
Hi-TRS [58]	39.1	63.3	70.7	42.9	68.3	74.8
CPM [46]	56.7	-	73.0	57.5	-	77.1
CMD [47]	50.6	71.0	75.4	53.0	75.3	80.2
HiCo [59]	54.4	-	73.0	54.8	-	78.3
PCM ³ [51]	53.8	-	<u>77.1</u>	53.1	-	<u>82.8</u>
UmURL [50]	<u>58.1</u>	<u>72.5</u>	-	<u>58.3</u>	<u>76.8</u>	-
C²VL (Ours)	69.3	79.4	81.8	69.1	82.1	85.5

its effectiveness and strong generalization capabilities in learning high-quality task-agnostic representations without relying on extensive labels.

4) *KNN Evaluation*: In this experiment, we utilize the K-nearest neighbors (KNN) as a classifier for action retrieval based on the obtained skeleton representation from the pre-training model. The results on NTU60 and NTU120 datasets are shown in Table IV. Our method achieves the best results among all tasks, surpassing the previous methods by a large margin. Moreover, it demonstrates that the obtained skeleton representation is more discriminative than other methods.

5) *Transfer Learning Evaluation*: We evaluate the transfer generalizability of the obtained skeleton representation in this part. Specifically, we use the model pre-trained on the NTU60 and NTU120 datasets to finetune the PKU-MMD II dataset. As shown in Table V, our method outperforms the competitors

TABLE IV

COMPARISON TO THE STATE-OF-THE-ART METHODS FOR ACTION RETRIEVAL WITH THE JOINT STREAM ON NTU RGB+D 60 AND NTU RGB+D 120 DATASETS. THE BEST AND SECOND-BEST RESULTS ARE HIGHLIGHTED IN **BOLD** AND UNDERLINED, RESPECTIVELY.

Method	NTU60		NTU120	
	xsub	xview	xsub	xset
LongT GAN [60]	39.1	48.1	31.5	35.5
P&C [61]	50.7	76.3	39.5	41.8
ISC [57]	62.5	82.6	50.6	52.3
AimCLR [39]	62.0	71.5	-	-
CMD [47]	70.6	85.4	58.3	60.9
HiCLR [62]	67.3	75.3	-	-
HiCo [59]	68.3	84.8	56.6	59.1
HaLP [48]	65.8	83.6	55.8	59.0
UmURL [50]	71.3	88.3	58.5	60.9
PCM ³ [51]	<u>73.7</u>	<u>88.8</u>	<u>63.1</u>	<u>66.8</u>
C²VL (Ours)	78.0	88.8	64.0	68.8

TABLE V

COMPARISON TO THE STATE-OF-THE-ART METHODS WITH TRANSFER LEARNING ON XSUB TASK. THE SOURCE DATASET IS NTU RGB+D 60 OR NTU RGB+D 120, AND THE TARGET DATASET IS PKU-MMD II. THE BEST AND SECOND-BEST RESULTS ARE HIGHLIGHTED IN **BOLD** AND UNDERLINED, RESPECTIVELY.

Method	Transfer to PKU-MMD II	
	NTU60	NTU120
LongT GAN [60]	44.8	-
M ² L [55]	45.8	-
ISC [57]	45.9	-
CrosSCLR [6]	54.0	52.8
CMD [47]	56.0	57.0
HiCo [59]	56.3	55.4
UmURL [50]	<u>58.2</u>	<u>57.6</u>
C²VL (Ours)	67.5	69.6

by a large margin, showing the excellent transferability of our learned skeleton representation, which has enormous potential in data-scarcity scenarios.

D. Evaluation of Knowledge Necessity

To further explore the significance of distinct modal information during the pre-training phase, we employed single-modal knowledge prompts as the supervision for pre-training. Table VI presents the action recognition accuracy of linear evaluation protocol across different modalities. Notably, vision-language knowledge prompts exhibit the best performance and offer valuable guidance and assistance for skeleton representation learning. In addition, language knowledge prompts tend to offer more fine-grained and local semantic details than vision knowledge prompts cannot provide.

E. Ablation Study

1) *Influences of Components*: We evaluate the efficiency of different components during the pre-training phase in Table VII. It is noted that the proposed soft targets are necessary as they can draw the unpaired data with high similarity closer, fostering more robust task-agnostic skeleton representations. Additionally, dynamic partitioning and progressive mechanisms have effectively controlled the degree of pair-bringing.

TABLE VI
ANALYSIS OF DIFFERENT KNOWLEDGE PROMPTS ON NTU RGB+D 60 XSUB DATASET WITH THE JOINT STREAM.

Knowledge		xsub	xview
Vision	Language		
✓	✗	78.6	81.9
✗	✓	83.8	88.6
✓	✓	84.4	89.8

TABLE VII
ANALYSIS OF DIFFERENT COMPONENTS ON NTU RGB+D 60 XSUB DATASET WITH THE JOINT STREAM.

Soft Targets		Contrastive Strategies		Acc (%)
Intra-Similarity	Inter-Consistency	Dynamic Partitioning	Progressive Control	
✗	✗	✗	✗	82.0
✓	✗	✗	✗	82.8
✗	✓	✗	✗	83.0
✓	✓	✗	✗	83.4
✓	✓	✓	✗	81.9
✓	✓	✗	✓	84.0
✓	✓	✓	✓	84.4

2) *Influences of Skeleton Encoders*: Furthermore, we analyze the performance of our method across different skeleton encoders, including GRU, GCN, and Transformer architectures. As shown in Table VIII, the GCN series encoders achieve the promised performance, which retains the topology structure of skeleton data and explores the spatial-temporal characteristic of actions. It is noted that the performance positively correlates with the ability of encoders. However, the results of UmURL drop a lot because its Transformer architecture decouples and impairs the spatial-temporal topology property of the skeleton. The PCM³ with GRU architecture neglects the spatial structure of the skeleton, resulting in inferior modeling of spatial movements. Therefore, our method can effectively guide the learning of skeleton representation from the complete topology skeleton.

3) *Influences of the Hyper-parameters*: As shown in Fig. 6, we evaluate the influence of the hyper-parameters. For the hyper-parameter α , we find that the teacher network should dominate the early learning period, and the progressive extent should be large for full exploration to align unpaired cross-modal data with high similarity. Meanwhile, the hyper-parameter β exhibits a slight increase and decrease, showing that the hard alignment and the robustness of our proposed

TABLE VIII
THE INFLUENCE OF DIFFERENT SKELETON ENCODERS ON NTU RGB+D 60 DATASET WITH THE JOINT STREAM.

Backbone	Architecture	NTU60	
		xsub	xview
PCM ³	GRU	74.1 (-10.3)	80.1 (-9.7)
UmURL	Transformer	79.0 (-5.4)	84.7 (-5.1)
MS-G3D	GCN	84.5 (+0.1)	89.9 (+0.1)
CTR-GCN	GCN	84.5 (+0.1)	90.4 (+0.6)
ST-GCN (Our used)	GCN	84.4	89.8

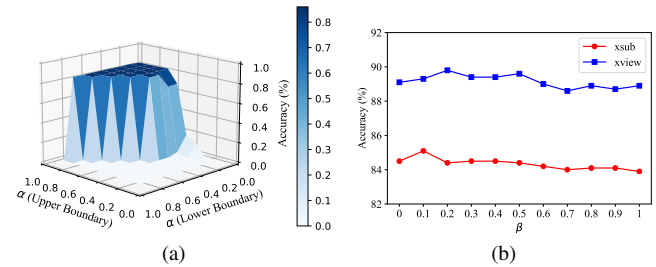


Fig. 6. (a) The influence of progressive extent α at different ratios on the NTU RGB+D 60 dataset. (b) The influence of intra-modal similarity guidance extent β at different ratios on the NTU RGB+D 60 dataset.

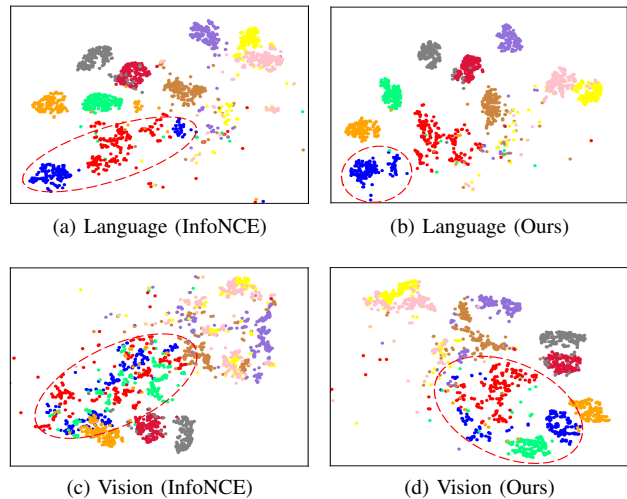


Fig. 7. The t-SNE visualization of action representations obtained by original InfoNCE loss (7a, 7c) and our proposed loss (7b, 7d) with the different modality as the supervision on the NTU RGB+D 60 xsub dataset. 10 classes from the testing set are randomly selected for visualization, where points of the same color correspond to the same action category.

intra-modal similarity guidance should be required.

F. Qualitative Analysis

1) *t-SNE Visualization of Representations*: We employed t-SNE [63] on the NTU RGB+D 60 xsub benchmark to visualize the embedding distribution obtained by InfoNCE loss and our proposed loss with vision and language knowledge prompts as supervision, respectively. As shown in Fig. 7, we select 10 classes for visualization, where points of the same color correspond to the same action category. It reveals that language provides better guidance for representations of discriminative skeletons than vision knowledge. Moreover, the proposed soft alignment and progressive self-distillation strategies have the advantage of clustering similar representations, resulting in better inter-class compactness and intra-class separability.

2) *Confusion Matrix*: Here, we draw the confusion matrices of skeleton-based action recognition results with the different modalities as the supervision based on InfoNCE loss and our proposed strategies. As shown in Fig. 8, we can find that the proposed soft alignment strategies significantly improve results, especially with the vision knowledge prompts as the supervision. Compared to the InfoNCE loss, our proposed loss improves recognition accuracy by nearly 10% with the

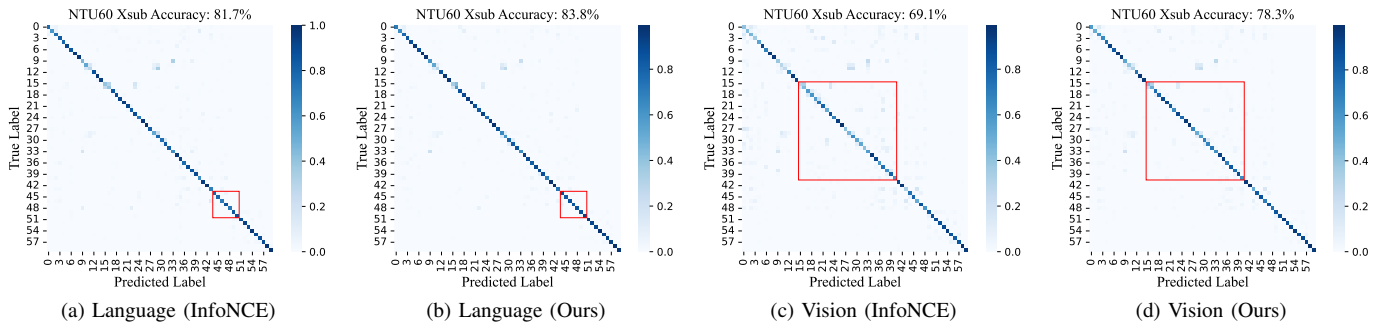


Fig. 8. The confusion matrices of original InfoNCE loss (8a, 8c) and our proposed loss (8b, 8d) with the different modality as the supervision on the NTU RGB+D 60 xsub dataset under the linear probe evaluation.

vision knowledge, demonstrating that aligning the high-similar unpaired data is necessary.

V. CONCLUSION

In this work, we propose a novel skeleton-based training paradigm with vision-language knowledge prompts as the supervision rather than extensive human-designed coarse-grained annotations. Leveraging large multimodal models, we generate the vision-language knowledge prompts to establish the vision-language action concept space, enriching the skeleton action space with fine-grained details. In addition, we design the intra-modal self-similarity and inter-modal cross-consistency softened targets to effectively control and guide the degree to which samples should be selectively pulled closer in the instance discrimination and knowledge distillation process. These noisy pairs come from the abovementioned action space consisting of vision-language prompts and their corresponding skeleton. During the inference phase, only the skeleton serves as the input for action recognition. Experimental results show that our method achieves superior performance and promises better skeleton action representations.

REFERENCES

- [1] F. Sato, R. Hachiuma, and T. Sekii, "Prompt-guided zero-shot anomaly action recognition using pretrained deep skeleton features," in *Proceedings of the IEEE/CVF Conference on Computer Vision and Pattern Recognition*, 2023, pp. 6471–6480.
- [2] Z. Zhang, "Microsoft Kinect sensor and its effect," *IEEE multimedia*, vol. 19, no. 2, pp. 4–10, 2012.
- [3] Y. Chen, Z. Zhang, C. Yuan, B. Li, Y. Deng, and W. Hu, "Channel-wise topology refinement graph convolution for skeleton-based action recognition," in *Proceedings of the IEEE/CVF international conference on computer vision*, 2021, pp. 13 359–13 368.
- [4] H.-g. Chi, M. H. Ha, S. Chi, S. W. Lee, Q. Huang, and K. Ramani, "Infogcn: Representation learning for human skeleton-based action recognition," in *Proceedings of the IEEE/CVF Conference on Computer Vision and Pattern Recognition*, 2022, pp. 20 186–20 196.
- [5] J. Lee, M. Lee, S. Cho, S. Woo, S. Jang, and S. Lee, "Leveraging spatio-temporal dependency for skeleton-based action recognition," in *Proceedings of the IEEE/CVF International Conference on Computer Vision (ICCV)*, October 2023, pp. 10 255–10 264.
- [6] L. Li, M. Wang, B. Ni, H. Wang, J. Yang, and W. Zhang, "3d human action representation learning via cross-view consistency pursuit," in *Proceedings of the IEEE/CVF conference on computer vision and pattern recognition*, 2021, pp. 4741–4750.
- [7] Y. Zhu, H. Han, Z. Yu, and G. Liu, "Modeling the relative visual tempo for self-supervised skeleton-based action recognition," in *Proceedings of the IEEE/CVF International Conference on Computer Vision*, 2023, pp. 13 913–13 922.
- [8] L. Lin, J. Zhang, and J. Liu, "Actionlet-dependent contrastive learning for unsupervised skeleton-based action recognition," in *Proceedings of the IEEE/CVF Conference on Computer Vision and Pattern Recognition*, 2023, pp. 2363–2372.
- [9] A. Radford, J. W. Kim, C. Hallacy, A. Ramesh, G. Goh, S. Agarwal, G. Sastry, A. Askell, P. Mishkin, J. Clark *et al.*, "Learning transferable visual models from natural language supervision," in *International conference on machine learning*. PMLR, 2021, pp. 8748–8763.
- [10] M. Wang, J. Xing, and Y. Liu, "Actionclip: A new paradigm for video action recognition," *arXiv preprint arXiv:2109.08472*, 2021.
- [11] W. Xiang, C. Li, Y. Zhou, B. Wang, and L. Zhang, "Generative action description prompts for skeleton-based action recognition," in *Proceedings of the IEEE/CVF International Conference on Computer Vision*, 2023, pp. 10 276–10 285.
- [12] S. Liu, Z. Zeng, T. Ren, F. Li, H. Zhang, J. Yang, C. Li, J. Yang, H. Su, J. Zhu *et al.*, "Grounding dino: Marrying dino with grounded pre-training for open-set object detection," *arXiv preprint arXiv:2303.05499*, 2023.
- [13] H. Liu, C. Li, Q. Wu, and Y. J. Lee, "Visual instruction tuning," in *NeurIPS*, 2023.
- [14] P. Wang, Z. Li, Y. Hou, and W. Li, "Action recognition based on joint trajectory maps using convolutional neural networks," in *Proceedings of the 24th ACM international conference on Multimedia*, 2016, pp. 102–106.
- [15] M. Liu, H. Liu, and C. Chen, "Enhanced skeleton visualization for view invariant human action recognition," *Pattern Recognition*, vol. 68, pp. 346–362, 2017.
- [16] J. Liu, A. Shahroudy, D. Xu, and G. Wang, "Spatio-temporal lstm with trust gates for 3d human action recognition," in *Computer Vision—ECCV 2016: 14th European Conference, Amsterdam, The Netherlands, October 11–14, 2016, Proceedings, Part III 14*. Springer, 2016, pp. 816–833.
- [17] P. Zhang, C. Lan, J. Xing, W. Zeng, J. Xue, and N. Zheng, "View adaptive recurrent neural networks for high performance human action recognition from skeleton data," in *Proceedings of the IEEE international conference on computer vision*, 2017, pp. 2117–2126.
- [18] Y.-F. Song, Z. Zhang, C. Shan, and L. Wang, "Constructing stronger and faster baselines for skeleton-based action recognition," *IEEE transactions on pattern analysis and machine intelligence*, vol. 45, no. 2, pp. 1474–1488, 2022.
- [19] S. Yang, J. Liu, S. Lu, M. H. Er, and A. C. Kot, "Skeleton cloud colorization for unsupervised 3d action representation learning," in *Proceedings of the IEEE/CVF International Conference on Computer Vision*, 2021, pp. 13 423–13 433.
- [20] W. Wu, Y. Hua, C. Zheng, S. Wu, C. Chen, and A. Lu, "Skeletonmae: Spatial-temporal masked autoencoders for self-supervised skeleton action recognition," in *2023 IEEE International Conference on Multimedia and Expo Workshops (ICMEW)*. IEEE, 2023, pp. 224–229.
- [21] Q. Zeng, C. Liu, M. Liu, and Q. Chen, "Contrastive 3d human skeleton action representation learning via crossmoco with spatiotemporal occlusion mask data augmentation," *IEEE Transactions on Multimedia*, 2023.
- [22] S. Xu, H. Rao, X. Hu, J. Cheng, and B. Hu, "Prototypical contrast and reverse prediction: Unsupervised skeleton based action recognition," *IEEE Transactions on Multimedia*, vol. 25, pp. 624–634, 2021.
- [23] M. Wang, X. Li, S. Chen, X. Zhang, L. Ma, and Y. Zhang, "Learning representations by contrastive spatio-temporal clustering for skeleton-based action recognition," *IEEE Transactions on Multimedia*, 2023.

- [24] X. Wang and Y. Mu, "Localized linear temporal dynamics for self-supervised skeleton action recognition," *IEEE Transactions on Multimedia*, 2024.
- [25] C. Jia, Y. Yang, Y. Xia, Y.-T. Chen, Z. Parekh, H. Pham, Q. Le, Y.-H. Sung, Z. Li, and T. Duerig, "Scaling up visual and vision-language representation learning with noisy text supervision," in *International conference on machine learning*. PMLR, 2021, pp. 4904–4916.
- [26] D. Aganian, M. Köhler, S. Baake, M. Eisenbach, and H.-M. Groß, "How object information improves skeleton-based human action recognition in assembly tasks," in *2023 International Joint Conference on Neural Networks (IJCNN)*. IEEE, 2023, pp. 01–09.
- [27] A. Mondal, S. Nag, J. M. Prada, X. Zhu, and A. Dutta, "Actor-agnostic multi-label action recognition with multi-modal query," in *Proceedings of the IEEE/CVF International Conference on Computer Vision*, 2023, pp. 784–794.
- [28] H. Zheng, H. Li, B. Shi, W. Dai, B. Wang, Y. Sun, M. Guo, and H. Xiong, "Actionprompt: Action-guided 3d human pose estimation with text and pose prompting," in *2023 IEEE International Conference on Multimedia and Expo (ICME)*. IEEE, 2023, pp. 2657–2662.
- [29] G. Tevet, B. Gordon, A. Hertz, A. H. Bermano, and D. Cohen-Or, "Motionclip: Exposing human motion generation to clip space," in *European Conference on Computer Vision*. Springer, 2022, pp. 358–374.
- [30] W. Wu, X. Wang, H. Luo, J. Wang, Y. Yang, and W. Ouyang, "Bidirectional cross-modal knowledge exploration for video recognition with pre-trained vision-language models," in *Proceedings of the IEEE/CVF Conference on Computer Vision and Pattern Recognition*, 2023, pp. 6620–6630.
- [31] S. S. Kalakonda, S. Maheshwari, and R. K. Sarvadevabhatla, "Actiongpt: Leveraging large-scale language models for improved and generalized action generation," in *2023 IEEE International Conference on Multimedia and Expo (ICME)*. IEEE, 2023, pp. 31–36.
- [32] J. Li, C. Xiong, and S. C. Hoi, "Learning from noisy data with robust representation learning," in *Proceedings of the IEEE/CVF International Conference on Computer Vision*, 2021, pp. 9485–9494.
- [33] F. Radenovic, A. Dubej, A. Kadian, T. Mihaylov, S. Vandenhende, Y. Patel, Y. Wen, V. Ramanathan, and D. Mahajan, "Filtering, distillation, and hard negatives for vision-language pre-training," in *Proceedings of the IEEE/CVF conference on computer vision and pattern recognition*, 2023, pp. 6967–6977.
- [34] A. Andonian, S. Chen, and R. Hamid, "Robust cross-modal representation learning with progressive self-distillation," in *Proceedings of the IEEE/CVF Conference on Computer Vision and Pattern Recognition*, 2022, pp. 16430–16441.
- [35] R. S. Srinivasa, J. Cho, C. Yang, Y. M. Saidutta, C.-H. Lee, Y. Shen, and H. Jin, "Cwcl: Cross-modal transfer with continuously weighted contrastive loss," *Advances in Neural Information Processing Systems*, vol. 36, 2023.
- [36] P. Morgado, I. Misra, and N. Vasconcelos, "Robust audio-visual instance discrimination," in *Proceedings of the IEEE/CVF Conference on Computer Vision and Pattern Recognition*, 2021, pp. 12934–12945.
- [37] Y. Gao, J. Liu, Z. Xu, T. Wu, E. Zhang, K. Li, J. Yang, W. Liu, and X. Sun, "Softclip: Softer cross-modal alignment makes clip stronger," in *Proceedings of the AAAI Conference on Artificial Intelligence*, vol. 38, no. 3, 2024, pp. 1860–1868.
- [38] H. Huang, Z. Nie, Z. Wang, and Z. Shang, "Cross-modal and uni-modal soft-label alignment for image-text retrieval," in *Proceedings of the AAAI Conference on Artificial Intelligence*, vol. 38, no. 16, 2024, pp. 18298–18306.
- [39] T. Guo, H. Liu, Z. Chen, M. Liu, T. Wang, and R. Ding, "Contrastive learning from extremely augmented skeleton sequences for self-supervised action recognition," in *Proceedings of the AAAI Conference on Artificial Intelligence*, vol. 36, no. 1, 2022, pp. 762–770.
- [40] A. v. d. Oord, Y. Li, and O. Vinyals, "Representation learning with contrastive predictive coding," *arXiv preprint arXiv:1807.03748*, 2018.
- [41] K. Kim, B. Ji, D. Yoon, and S. Hwang, "Self-knowledge distillation with progressive refinement of targets," in *Proceedings of the IEEE/CVF international conference on computer vision*, 2021, pp. 6567–6576.
- [42] T. Li, J. Li, Z. Liu, and C. Zhang, "Few sample knowledge distillation for efficient network compression," in *Proceedings of the IEEE/CVF conference on computer vision and pattern recognition*, 2020, pp. 14639–14647.
- [43] A. Shahroudy, J. Liu, T.-T. Ng, and G. Wang, "Ntu rgb+ d: A large scale dataset for 3d human activity analysis," in *Proceedings of the IEEE conference on computer vision and pattern recognition*, 2016, pp. 1010–1019.
- [44] J. Liu, A. Shahroudy, M. Perez, G. Wang, L.-Y. Duan, and A. C. Kot, "Ntu rgb+ d 120: A large-scale benchmark for 3d human activity understanding," *IEEE transactions on pattern analysis and machine intelligence*, vol. 42, no. 10, pp. 2684–2701, 2019.
- [45] L. Chunhui, H. Yueyu, L. Yanghao, S. Sijie, and L. Jiaying, "Pku-mmd: A large scale benchmark for continuous multi-modal human action understanding," *arXiv preprint arXiv:1703.07475*, 2017.
- [46] H. Zhang, Y. Hou, W. Zhang, and W. Li, "Contrastive positive mining for unsupervised 3d action representation learning," in *European Conference on Computer Vision*. Springer, 2022, pp. 36–51.
- [47] Y. Mao, W. Zhou, Z. Lu, J. Deng, and H. Li, "Cmd: Self-supervised 3d action representation learning with cross-modal mutual distillation," in *European Conference on Computer Vision*. Springer, 2022, pp. 734–752.
- [48] A. Shah, A. Roy, K. Shah, S. Mishra, D. Jacobs, A. Cherian, and R. Chellappa, "Halp: Hallucinating latent positives for skeleton-based self-supervised learning of actions," in *Proceedings of the IEEE/CVF Conference on Computer Vision and Pattern Recognition*, 2023, pp. 18846–18856.
- [49] S. Guan, X. Yu, W. Huang, G. Fang, and H. Lu, "Dmmg: Dual min-max games for self-supervised skeleton-based action recognition," *IEEE Transactions on Image Processing*, 2023.
- [50] S. Sun, D. Liu, J. Dong, X. Qu, J. Gao, X. Yang, X. Wang, and M. Wang, "Unified multi-modal unsupervised representation learning for skeleton-based action understanding," in *Proceedings of the 31st ACM International Conference on Multimedia*, 2023, pp. 2973–2984.
- [51] J. Zhang, L. Lin, and J. Liu, "Prompted contrast with masked motion modeling: Towards versatile 3d action representation learning," in *Proceedings of the ACM International Conference on Multimedia*, 2023.
- [52] S. Yan, Y. Xiong, and D. Lin, "Spatial temporal graph convolutional networks for skeleton-based action recognition," in *Proceedings of the AAAI conference on artificial intelligence*, vol. 32, no. 1, 2018.
- [53] K. Cheng, Y. Zhang, X. He, W. Chen, J. Cheng, and H. Lu, "Skeleton-based action recognition with shift graph convolutional network," in *Proceedings of the IEEE/CVF conference on computer vision and pattern recognition*, 2020, pp. 183–192.
- [54] C. Si, X. Nie, W. Wang, L. Wang, T. Tan, and J. Feng, "Adversarial self-supervised learning for semi-supervised 3d action recognition," in *Computer Vision—ECCV 2020: 16th European Conference, Glasgow, UK, August 23–28, 2020, Proceedings, Part VII 16*. Springer, 2020, pp. 35–51.
- [55] L. Lin, S. Song, W. Yang, and J. Liu, "Ms2l: Multi-task self-supervised learning for skeleton based action recognition," in *Proceedings of the 28th ACM International Conference on Multimedia*, 2020, pp. 2490–2498.
- [56] Y. Su, G. Lin, and Q. Wu, "Self-supervised 3d skeleton action representation learning with motion consistency and continuity," in *Proceedings of the IEEE/CVF international conference on computer vision*, 2021, pp. 13328–13338.
- [57] F. M. Thoker, H. Doughty, and C. G. Snoek, "Skeleton-contrastive 3d action representation learning," in *Proceedings of the 29th ACM international conference on multimedia*, 2021, pp. 1655–1663.
- [58] Y. Chen, L. Zhao, J. Yuan, Y. Tian, Z. Xia, S. Geng, L. Han, and D. N. Metaxas, "Hierarchically self-supervised transformer for human skeleton representation learning," in *European Conference on Computer Vision*. Springer, 2022, pp. 185–202.
- [59] J. Dong, S. Sun, Z. Liu, S. Chen, B. Liu, and X. Wang, "Hierarchical contrast for unsupervised skeleton-based action representation learning," in *Proceedings of the AAAI Conference on Artificial Intelligence*, vol. 37, no. 1, 2023, pp. 525–533.
- [60] N. Zheng, J. Wen, R. Liu, L. Long, J. Dai, and Z. Gong, "Unsupervised representation learning with long-term dynamics for skeleton based action recognition," in *Proceedings of the AAAI Conference on Artificial Intelligence*, vol. 32, no. 1, 2018.
- [61] K. Su, X. Liu, and E. Shlizerman, "Predict & cluster: Unsupervised skeleton based action recognition," in *Proceedings of the IEEE/CVF Conference on Computer Vision and Pattern Recognition*, 2020, pp. 9631–9640.
- [62] J. Zhang, L. Lin, and J. Liu, "Hierarchical consistent contrastive learning for skeleton-based action recognition with growing augmentations," in *Proceedings of the AAAI Conference on Artificial Intelligence*, vol. 37, no. 3, 2023, pp. 3427–3435.
- [63] L. Van der Maaten and G. Hinton, "Visualizing data using t-sne," *Journal of machine learning research*, vol. 9, no. 11, 2008.